Moving with bubbles: a review of the interactions between bubbles and the microorganisms that surround them

Published in: Integrative and Comparative Biology, 54(6): 1014 (2014). DOI: 10.1093/icb/icu100

Peter L. L. Walls¹, James C. Bird^{1*}, and Lydia Bourouiba^{2*}

Synopsis Bubbles are ubiquitous in biological environments, emerging during the complex dynamics of waves breaking in the open oceans or being intentionally formed in bioreactors. From formation, through motion, until death, bubbles play a critical role in the oxygenation and mixing of natural and artificial ecosystems. However, their life is also greatly influenced by the environments in which they emerge. This interaction between bubbles and microorganisms is a subtle affair in which surface tension plays a critical role. Indeed, it shapes the role of bubbles in mixing or oxygenating microorganisms, but also determines how microorganisms affect every stage of the bubble's life. In this review, we guide the reader through the life of a bubble from birth to death, with particular attention to the microorganism-bubble interaction as viewed through the lens of fluid dynamics.

1. Introduction

The Red tide events associated with algal blooms are among the first examples of phenomena in which bioaerosols were linked to oceanic bursting bubbles. To form the link, Woodcock (1948) sprayed aerosolized seawater containing marine microorganisms into the nose and throat of volunteers, who subsequently developed symptoms respiratory irritation analogous to those observed in residents of shorelines. Such correlation effectively solidified the earlier hypothesis on the role of bubbles in the creation of marine aerosols (Stuhlman 1932; Jacobs 1937; Woodcock et al. 1953).

In subsequent years, sea spray aerosols have been shown to originate mostly from the bubbles within the foam generated by breaking waves (Boyce 1951; Blanchard (Fig. 1a). Diseases associated with 1963) bursting bubbles are now linked to various pathogen-bearing pools of water such as recreational swimming pools (Falkinham III 2003), hot tubs (Parker et al. 1983; Embil et al. 1997), or wastewater treatment plants (Bauer et al. 2002; Laitinen et al. 1994). Bubbles are, in fact, ubiquitous in biology (Bourouiba & Bush 2012), being responsible for mixing and aeration in the upper layer of the ocean (Blanchard 1989), cell mortality in bioreactors from direct injection aeration (referred to as

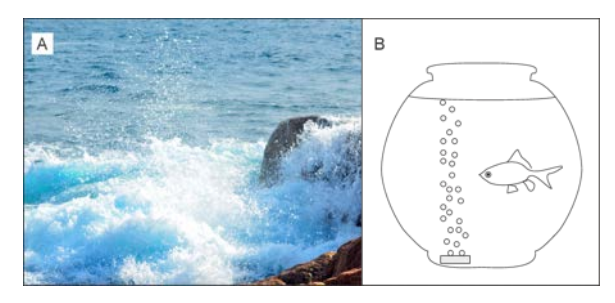


Figure 1. A) Wave breaking illustrating the formation of a spectrum of bubbles commonly referred to as white caps. B) Bubbles may also be deliberately injected into a closed container to aerate the liquid.

sparging) (Barbosa et al. 2003; Hu et al. 2011) and rupture at the surface (Murhammer & Goochee 1990; Chisti 2000), for example.

While bubbles play an important role in a variety of biological systems, our review highlights the physical processes shaping the life of a bubble and its interaction with its biological environment: from its birth in the fluid bulk to its rupture at the fluid surface. We pay particular attention to the contexts of open oceans (Fig. 1A) and closed biological environments (Fig. 1B). In the ocean, the breaking of waves is a ubiquitous process that entrains air and creates bubbles. These bubbles are critical for the healthy functioning and mixing of the ecosystems of the upper

¹ Department of Mechanical Engineering, Boston University; ² Department of Civil and Environmental Engineering, Massachusetts Institute of Technology, Cambridge, 02139

^{*} E-mails: jbird@bu.edu, lbouro@mit.edu

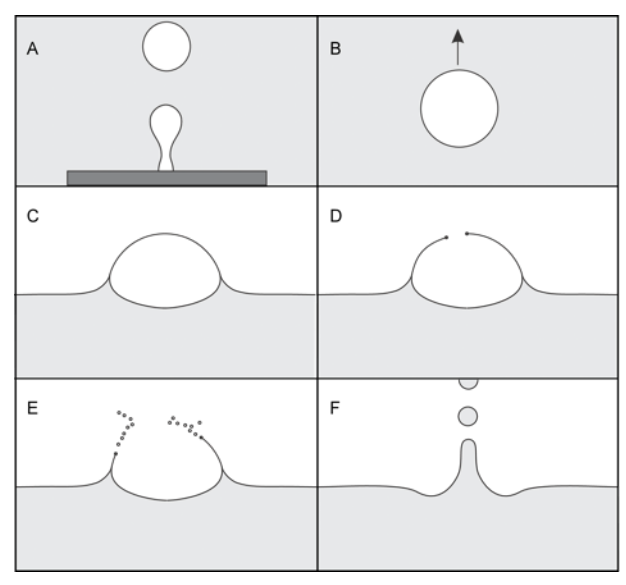


Figure 2. Various stages in the life of a bubble: **A**) formation, **B**) rise and dissolution, **C**) drainage once at free surface, **D**) holenucleation and film-retraction, **E**) production of film drops,, and **F**) production of a jet and jet drops.

surface of the ocean. Similarly, direct and continuous injection of air is vital to the aeration of most bioreactors so as to provide proper oxygenation of their live content (cells or other living forms such as fish). However, the large stresses induced by constant injection of gas can also potentially be detrimental to the health of the cell populations (e.g. Garcia-Briones & Chalmers 1994; Liu et al. 2013)

Once the bubble is formed (Fig. 2A), it begins to rise as a consequence of the gas in the bubble being less dense than the surrounding liquid. While rising, bubbles interact with the surrounding liquid (Bhaga & Weber 1981). The bubble might continue to rise until it reaches the free surface, or alternatively it might completely dissolve into the ambient fluid during its journey. Regardless of its fate, the rising bubble is an efficient biological mixer. Not only is ambient fluid transported in its wake, but also, the bubble can mix the water via the shedding of vortices that can spread laterally (Magnaudet & Eames 2000). bubble Moreover. а can scavenge microorganisms and particles (e.g. viruses, bacteria, cells, and toxins) on its surface, resulting in their passive transport. When reaching the surface (Fig. 2C), the thin film that defines the bubble's boundary drains due to gravitational and capillary forces, until it eventually becomes sufficiently thin for a nucleating hole to grow, the film to retract, and the bubble to pop (Fig. 2D). The retracting film can fragment into numerous film-droplets (Fig. 2E) that can persist well after the bubble is gone. Lastly, jet droplets often are created from a jet that forms when the air cavity, that was once the bubble, rapidly equilibrates with its surroundings (Fig. 2F).

Due to the life history of the bubble through the water column, the droplets that it produces can end up being enriched in their content of microorganisms and particles. containing higher concentration particulates than that of the bulk fluid that the bubble traversed (Blanchard & Syzdek 1970). In turn, the nature of the particles or organisms, their size, shape, and surface properties can change the life of a bubble by fundamentally altering its surface hydrodynamic properties, in addition to more directly also changing its gas content through consumption.

We have structured this review by following a bubble's life history from its inception (Fig 2A, section 3), throughout its journey through the biological world (Fig 2B, section 4), to its final destination and rupture (Fig 2C-D, section 5) and we close by discussing its legacy in the form of residual droplets (Fig 2E-F, section 6). We aim at presenting these events to an audience that may be less familiar with the concepts of surface tension and fluid mechanics in general and so start by introducing such general concepts in section 2.

2. Origin and relevance of capillarity

When two fluids are immiscible, such as water and air, the molecules in each fluid are more attracted to like molecules than to the other type. The consequence of this difference in attraction is that work is required to increase the surface area at the interface of the two

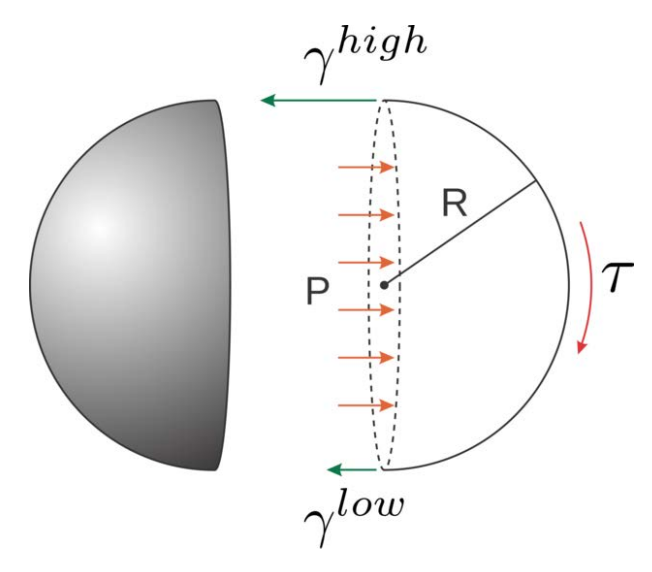


Figure 3: Illustration of the balance of capillary force and internal pressure force. τ represents the interfacial stress acting on the bubble's surface resulting from the fluid's resistance to the bubble's motion. The imbalance of the surface tensions γ^{high} and γ^{low} will cause a motion of the interface known as Marangoni flow in an attempt to restore balance.

fluids. The amount of energy ΔE needed to increase the surface area by ΔA is determined by the surface tension γ , such that $\Delta E = \gamma \Delta A$. Therefore surface tension can be interpreted as energy per unit area, or force per unit length. In this review, forces resulting from surface tension will be referred to as capillary forces, or capillarity.

A spherical bubble with radius R has been schematically split apart in Figure 3. Surface tension can be interpreted as the amount of tension being applied to the surface: thus, if a force balance were drawn over half of the bubble, the surface tension would manifest itself as a tangential force per unit length acting along the bubble's perimeter (leftward arrows in Fig. 3). If the bubble were in mechanical equilibrium, the balance of forces implies that there must be a pressure Ppushing back against the internal face of the bubble (rightward arrows in Fia.

Specifically, the product of the perimeter $2\pi R$ and the average surface tension γ must be equal to the product of the area πR^2 and this pressure P. This force balance leads to $P=2\gamma/R$, highlighting that the inner pressure of the bubble is higher than that outside by a capillary pressure value P that increases with surface tension and decreases with radius. In other words, for the same surface tension γ a small bubble would have a higher inner pressure than a larger bubble. For the same radius R a bubble made of an interface with a higher surface tension γ would have a higher inner pressure than that with a lower surface-tension interface.

Surface tension can also vary spatially due to thermal or chemical gradients. For example, certain bacteria are known to excrete surfactants that locally reduce surface tension (e.g. Angelini et al. 2009). A gradient of surface tension can thus be generated, resulting in a reactive motion on such an interface. Such motion, referred to as Marangoni flow (Marangoni 1865; Scriven & Sternling 1960) is directed from low γ^{low} to high γ^{high} regions of surface tension; thus redistributing surfactants and effectively opposing the mechanism of generating a gradient of surfactant (Berg et al. 1966; Hosoi & Bush 2001). In Figure 3 the concentration of surfactants is higher at the bottom of the bubble than at the top. The force balance illustrates that a torque or moment is then generated, resulting in a tangential stress (Clift et al. 1978). At equilibrium, this Marangoni stress is countered by an equal and opposite applied stress τ (as shown Fig. 3).

In general, elements of a bubble are dynamic rather than static. This motion is governed by Newton's second law, which can be reexpressed in the form of the classical Navier-Stokes equation when accounting for the fluid forces involved:

$$\rho \left(\frac{\partial \mathbf{u}}{\partial t} + \mathbf{u} \cdot \nabla \mathbf{u} \right) = -\nabla p + \mu \nabla^2 \mathbf{u} + \Delta \rho \mathbf{g}. \tag{0.0}$$

Here ρ is the density of the gas and $\Delta \rho = \rho - \rho_{\rm g}$ is the difference between the density of gas in the bubble and the density of the surrounding fluid $\rho_{\rm a}$, ${\bf u}$ is the velocity, μ is the dynamic viscosity, and ${\bf g}$ is the gravitational acceleration. The left-hand side of Eq. (2.1) is the expanded expression of the mass times acceleration for a unit volume; while the right-hand side is the expression of the sum of the forces acting on such unit volume.

For all equations governing physical systems, the dimensions of each term need to be equivalent. It is helpful in both physical and mathematical analysis to non-dimensionalize the equations of motion. This is particularly true in fluid dynamics where the use of dimensionless parameters can also give insight into the physical processes taking place. The relevant dimensionless groups naturally emerge when non-dimensionalizing Eq. (2.1). This process involves first identifying characteristic scales in the system being examined, such as a characteristic length L or velocity $\boldsymbol{u}_{\boldsymbol{c}}$. Each variable is then nondimensionalized. For example. the dimensional length variable x (or y or z) can be normalized by a characteristic scale of length $\boldsymbol{L}_{,}$ leading to a non-dimensional length variable $\tilde{x} = x/I$. Here, we follow the convention of denoting non-dimensional variables with a tilde. Similarly, we can construct a non-dimensional velocity $\tilde{\mathbf{u}} = \mathbf{u} / \mathbf{u}$ and time $\tilde{\tau} = u_{,t}/L$. A natural choice for the characteristic pressure is the capillary pressure, such that $\tilde{p} = pL/\gamma$. Rewriting Eq. (2.1) in terms of these non-dimensional variables with the pressure term pre-factor of unity leads to

$$We\left(\frac{\partial \tilde{\mathbf{u}}}{\partial \tau} + \tilde{\mathbf{u}} \cdot \tilde{\nabla} \tilde{\mathbf{u}}\right) = -\tilde{\nabla} \tilde{\mathbf{p}} + Ca\tilde{\nabla}^2 \tilde{\mathbf{u}} + Bo\hat{\mathbf{z}}, \tag{0.0}$$

where three dimensionless parameters emerge. The Weber number $We\,{=}\,\rho u_c^2 L\,/\gamma$ quantifies the relative importance of inertial

and capillary forces. The capillary number $Ca=\mu u_{\rm c}/\gamma$ quantifies the relative importance of viscous and capillary forces, and the Bond number

$$Bo = \Delta \rho g L^2 / \gamma \tag{0.0}$$

quantifies the relative importance of gravitational and capillary forces. Furthermore, if one or more of these dimensionless parameters is significantly smaller than the others, those terms in Eq. (2.2) do not contribute significantly to the dominant dynamics; thus can be dropped, thereby simplifying the first-order analysis.

Perhaps the most famous dimensionless number in fluid mechanics is the Reynolds number

$$Re = \rho u_c L/\mu, \qquad (0.0)$$

which quantifies the relative balance of inertial and viscous effects. Quick inspection reveals that the Weber and capillary numbers can be related to the Reynolds number by We/Ca=Re.

In some interfacial flows, the characteristic velocity is not imposed, but instead is established, based on a balance of underlying forces. For example, when capillary and inertial forces balance We=1, which occurs when $u_{\rm c}=\sqrt{\gamma/\rho L}$. Substituting this characteristic velocity into Eq. (2.4) yields the Ohnesorge number $Oh=\mu/\sqrt{\rho\gamma L}$, a number that quantifies the relative importance of viscous and inertial effects in capillary flows. In this case, (2.2) reduces to

$$\frac{\partial \tilde{\mathbf{u}}}{\partial \tau} + \tilde{\mathbf{u}} \cdot \tilde{\nabla} \tilde{\mathbf{u}} = -\tilde{\nabla} \tilde{\mathbf{p}} + \mathrm{Oh} \tilde{\nabla}^2 \tilde{\mathbf{u}} + \mathrm{Bo} \hat{\mathbf{z}}. \tag{0.0}$$

Here the flow regime is determined by two dimensionless parameters: Oh and Bo.

The subsequent sections rely on the physical framework above to describe the interactions between a bubble and its surrounding biological environment. Throughout a

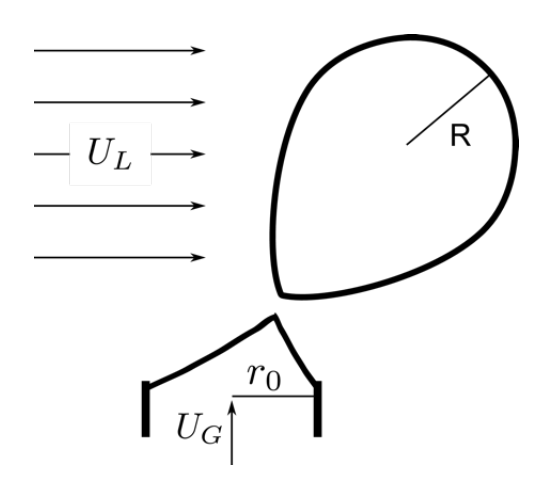


Figure 4. Illustration of gas bubble with radius R being pinched-off at an orifice submerged in a liquid with cross-flow.

bubble's life, the capillary forces can attract, stress, and disperse surrounding biomaterial. Similarly, this biomaterial can modify the capillary forces through, for example, producing or acting as a surfactant. When appropriate, our discussion will incorporate the concepts outlined in Figure 3 and the dimensionless numbers presented in this section.

3. A bubble is born

Bubbles are ubiquitous across natural bodies of water, such as ponds, lakes, and oceans. These bubbles may be formed in any process that breaks the interface and entrains air into the water (Blanchard 1989), including rainfalls, snowfalls, and breaking waves. Here, we focus on breaking waves, as they are more common than rainfalls and snowfalls around the globe. Waves not only break at the shore (Fig. 1A), but also in the middle of the ocean when wind speeds are high enough to destabilize the surface waves (typically above 3 m/s (Blanchard 1963; Monahan 1971)). The breaking and the formation of whitecaps dissipate surface-wave energy and generate the mixing of gas and biomaterial via turbulence and bubble-entrainment (Melville 1996). Typically, whitecaps consist of a myriad of small bubbles rising to the surface. The size of such bubbles are estimated to range from

micrometers to centimeters (Blanchard & Woodcock 1957; Baldy S. & Bourguel 1987; Deane & Stokes 2002). Recent studies examined the spectrum of bubble-sizes (number of bubbles per m^3 per μm radius increment) generated early in the breaking of a wave and found two power-law scalings The transition between these two scalings occurs at $R \approx 1$ mm in seawater and is related to the level of the rate of dissipation of turbulence. Small bubbles are subject to the stabilization of surface tension and scale as $R^{-3/2}$, while larger bubbles are subject to turbulence and shear, leading to frequent breakups that scale as $R^{-10/3}$ (Deane & Stokes 2002).

In artificial bodies of water, bubbles are created for aeration. While other options for maintaining dissolved gas levels of oxygen and carbon dioxide (e.g. surface aeration) are available in small-scale bioreactors, direct injection of gas is essential when production scales are involved. Yet, there are some undesirable consequences; sparging has been shown in recent studies to have detrimental effects on cells near the region of bubble formation (Barbosa et al. 2003; Zhu et al. 2008; Liu et al. 2013). A widely used scalar parameter for quantifying cell damage in incompressible Newtonian fluids is the energydissipation rate ϵ (Liu et al. 2013). Ma et al. (2002) examined a variety of cells of industrial relevance and found that energy-dissipation rates of 10-100 W/cm³ caused as many as 20% of the more sensitive cells to be damaged, specifically the mammalian cells which lack a protective cell wall. Such values are orders of magnitude higher than those achieved in a mixed tank (Wernersson & Trägårdh 1999), but are comparable to the energy dissipation of small bursting bubbles (Boulton-Stone & Blake 1993). Following the method of Cherry & Hulle (1992) we can estimate the energy dissipation as:

$$\varepsilon = \frac{1}{\pi r_{\text{rim}}^2} \left(\frac{2\gamma^3}{\rho h} \right)^{1/2}$$

with $r_{\rm rim}$ the radius of the retracting rim and h the bubble thickness (see section 5). For example, a water bubble with a radius of 1 mm and thickness of 10 μm yields an energy dissipation of 52 W/cm^3 . While excessive hydrodynamic stresses are agreed to be one of the main causes for cell damage (Tramper et al. 1986; Garcia-Briones & Chalmers 1994), no model is able to relate the hydrodynamic forces to lethal and non-lethal cell effects (Hu et al. 2011).

In sparged systems, the formation of a bubble occurs at an orifice via a complex process depending on the fluid's properties, the orifice's geometry, and the conditions of the surrounding flow (Kumar & Kuloor 1970; Miyahara & Hayashino 1995; Thoroddsen et al. 2007). However, in the simple case of slow injection of gas into a stagnant fluid we can approximate the bubble's radius by balancing the capillary $F_{\rm c}=2\pi r_{\rm 0}\gamma$ and buoyancy forces $F_b = \frac{4}{3}\pi\Delta\rho g R^3$. By setting Bo = 1 based on the orifice's radius (r_0 in Fig. 4) the resulting radius of the bubble becomes $R = 1.14r_0 \approx l_c$, in which $l_c = \sqrt{\gamma/\Delta\rho g}$ is the capillary length. The capillary length is the length scale at which gravitational and capillary effects are effectively balanced. For air surrounded by water, or alternatively water droplets surrounded by air, the capillary length is $1_{s} \approx 2 \text{mm}$.

stirred bioreactors. in environments, the fluid surrounding bubbles is not stagnant but instead flows over the bubble-generating orifice (Fig. 4). This crossflow exerts an additional force on the bubble leading to a shift of its detachment from being buoyancy-dominated to shear-dominated. This shearing force will encourage detachment from the orifice, resulting in smaller bubbles being produced frequently than in the case of stagnant fluid. Not only does a cross-flow reduce the size of bubbles exiting from a single orifice, but it also reduces the frequency of coalescence among

adjacent bubbles in closely spaced orifices like those commonly found on spargers. Ultimately, a more uniform and predictable distribution of bubble sizes can be produced (Maier 1927; Sullivan et al. 1964).

4. A bubble's journey upwards

The purpose of sparging and other types of aeration techniques is to control the level of a dissolved gas in a life-supporting fluid medium. As a bubble rises, mass transfer occurs at its interface. The mass transfer rate j_b is driven by the difference in gas concentration between the inner and outer the regions of bubble. $j_b = 4\pi R^2 k_L (c_b - c_\infty)$, where c_b and c_∞ are the concentrations of gas in the bubble and surrounding fluid, and $k_{\scriptscriptstyle L}$ is the mean mass transfer coefficient(Gong et al. 2007). The concentration of dissolvable gas in the bubble is related to the partial pressure of the gas inside p_h through henry's law:

$$p_b = Hc_b$$

Here the henry constant H has units of $\frac{L \cdot atm}{mg}$ and is experimentally determined for specified combinations of liquid and gas at a fixed temperature. The mass change inside the bubble $j_b = \frac{d}{dt} \left(\frac{4}{3} \pi R^3 \rho_g \right)$ can be simplified to $j_b \approx 4\pi R^2 \rho_G \frac{dR}{dt}$ as contribution from the second term containing $\frac{d\rho_G}{dt}$ was shown experimentally to be less than 2% and can be neglected (Takemura & Yabe 1999). Equating these relations and utilizing the ideal gas law yields an expression for the rate at which a bubble shrinks as it dissolves:

$$\frac{dR}{dt} = \frac{p_b - p_{\infty}}{p_b} \frac{\Re Tk_L}{H}$$
 (4.1)

 $p_{\scriptscriptstyle \infty}$ here is the equivalent pressure of the dissolved gas in the liquid, \Re is the specific gas constant, and T is the absolute temperature.

An interesting result of Eq. (4.1) is that a bubble will be driven to dissolve even when the surrounding fluid is saturated due to the capillary pressure increase. While small bubbles with high internal pressure favor dissolution, observations have shown that bubbles with $R < 60 \mu m$ mav indefinitely in the ocean (Mulhearn 1981). This phenomenon has been attributed to the bubbles being coated with natural surfactants, thereby inhibiting mass transfer (Czerski et al. 2011). The primary source of these surfactants appears to be phytoplankton exudates (Zutić et al. 1981; Wurl et al. 2011).

The rise of a bubble through its surroundings is driven by the buoyancy force F_b (Section 2) and is resisted by the fluid leading to an interfacial stress (τ in Fig. 3). For example, a bubble dominated by viscosity and surface tension, specifically small Re and Bo numbers, rising in an ideally clean fluid will be approximately spherical and possess a mobile interface. The fluid inside the bubble will move toroidally while the surrounding fluid will diverge and re-convergent behind the bubble to allow its passage as shown in Figure 5. In this case, the terminal rise velocity is given by the Hadamard-Rybczynski equation (Rybczynski 1911; Hadamard 1911):

$$\frac{u_{t}}{u_{c}} = \frac{2}{9} \operatorname{Re} \left(1 - \frac{\rho_{g}}{\rho_{l}} \right) \left(\frac{1 + \frac{\mu_{l}}{\mu_{g}}}{1 + \frac{2}{3} \frac{\mu_{l}}{\mu_{g}}} \right) (4.2)$$

wherein the characteristic velocity $u_{\rm c}=\sqrt{gR}$ is now given in terms of gravity, the driving force behind the bubble's rise. For an air bubble in water Eq. (4.2) can be simplified to $\frac{u_{\rm t}}{u_{\rm c}}=\frac{1}{3}\,Re$ owing to the large density and viscosity differences. However, as the bubble rises, the liquid encountered is rarely pure and instead filled with suspended particles, such as viruses and microorganisms. When such surfactants are present in the fluid, they end up being scavenged by the rising bubble. Such scavenging leads to local changes of

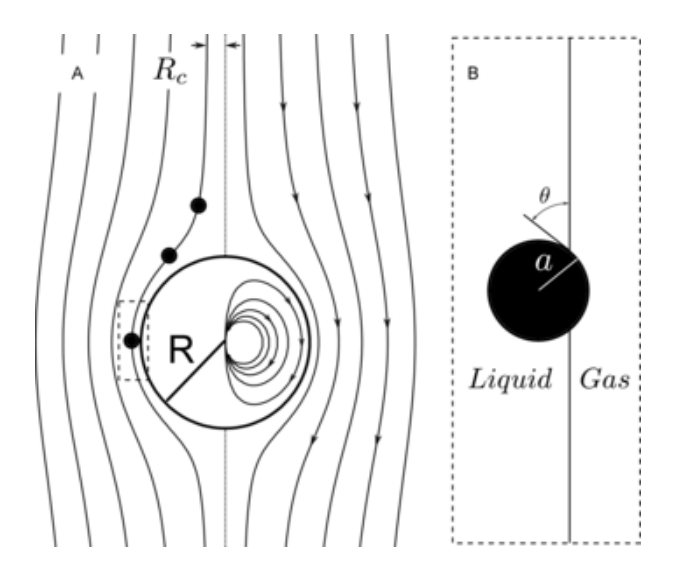


Figure 5. The rise of a spherical bubble in a fluid. A, illustrates on the right half the rise of a bubble in a clean environment. The left half illustrates a rigid interface with a particle contacting and adhering. B, close-up view of boxed particle in A that has formed a three-phase contact angle θ .

surface tension on the rising bubble's surface. The Marangoni stresses induced by such gradients resist the motion of the interface towards the back of the bubble, thus rendering the bubble's surface nearly immobile. The surface of the bubble behaves in a more rigid way.

In such cases, $\mu_{\rm g}\gg\mu_{\rm l}$ and Eq. (4.2) limits to the familiar Stoke's law $\frac{u_{\rm t}}{u_{\rm c}}=\frac{2}{9}\,{\rm Re}$ (Clift et al. 1978).Thus, smallerbubbles with surface

contamination dwell in the water approximately 50% longer than surfactant free bubbles.

As a bubble approaches a suspended particle, the particle will either pass around, or collide with, the bubble's surface (Fig. 5A). In the event of a particle-bubble collision it is possible for the particle not to attach

permanently to the free surface (Miettinen et al. 2010). For attachment to occur, the liquid between the particle and the thin bubble film must completely drain to allow for a threephase contact line to develop (Fig. 5B) (Verrelli et al. 2011). The time required for this process to occur is known as the induction time and must be less than the time required for the particle to simply "slide" around and off the back of the bubble. The induction time is influenced predominantly bv surface chemistry, although few experimental studies have thoroughly examined this phenomenon as it naturally occurs (Verrelli et al. 2011).

In the event of attachment upon particle-bubble collision (Fig. 5A) the concentration of particles at the surface of the rising bubble will become enriched when compared to that of the fluid bulk (Blanchard & Syzdek 1970; Blanchard & Syzdek 1972; Wallace et al. 1972; Blanchard & Syzdek 1982; Burger & Bennett 1985). Such effect can be quantified with the collision efficiency as defined by the ratio of particles attached to the bubble at the surface to the total number of particles in the volume swept out by the bubble during its rise

$$E_{col} = \frac{\text{#of particles attached}}{\text{#of particles in volume swept}}$$
 (0.0)

Numerous factors can influence the collision efficiency, including particle-to-bubble size ratio, the mobility of the bubble's surface, and the hydrophobicity or hydrophilicity of the particle (Yoon & Luttrell 1989; Dai et al. 2000). Perhaps one of the simplest models of bubbleparticle collision assumes that the particle's inertia can be neglected owing to their small size, thus allowing them to follow the flow streamlines, as illustrated in Figure 5A, and enabling estimation of the number collisions. This model assumes that the Reynolds number of the bubble is sufficiently high, as opposed to Stoke's law case, to allow for the neglect of viscous or rotational effects, and that the bubble's surface is fully mobile (Sutherland 1948). This particular model applies when the Reynolds number is between

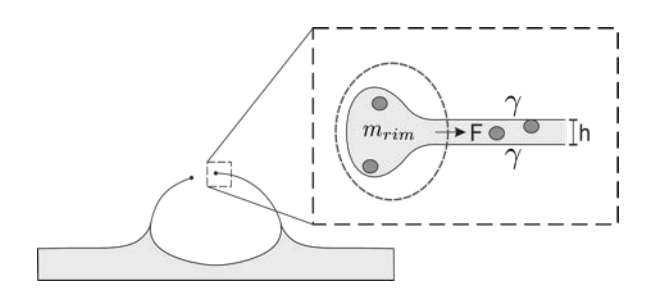


Figure 6. As a hole opens in the rupturing bubble, the liquid film is collected into a growing rim. Capillary driving forces balance inertial forces in such a way that the velocity of the retracting rim is nearly constant. As is seen in the boxed section, there are two liquid-gas interfaces (indicated by γ on the top and bottom)

80 and 500. Given such assumptions, a distance from the bubble's center-line $R_{\rm c}$ under which all particles will collide and attach can be derived $R_{\rm c}=\sqrt{3aR}$ (Fig. 5A). The collision efficiency $E_{\rm col}$ can then be computed via Eq. (3.1). By taking the ratio of the collision tube's area $3\pi aR$ to the projected area of the bubble πR^2 , the collision efficiency simplifies to $E_{\rm col}=3a/R$.

Despite the numerous assumptions built into the model above, the Sutherland collision efficiency has provided the foundation for many recent collision models (e.g. Dai et al. 2000). However, numerous factors can lead to the breakdown of the most fundamental assumptions. In particular, as discussed above, the mobility of the surface needs revision. In fact, an immobile surface always results in a lower collision efficiency owing to the fluid streamlines being forced away from the interface (Schulze 1992). More recent models of bubble-particle collision relaxed some of Sutherland's (1948) assumptions and were used to explain the enrichment of cells and bacteria attached to rising bubbles (Weber et al. 1983; Meier et al. 1999).

5. A bubble drains and dies

When a gas bubble rises to the surface of a liquid, it deforms the air-liquid interface. Toba (1959) and Princen (1963) independently reasoned that, at the fluid's interface, these bubbles reach an equilibrium shape that depends on the relative effects of gravity and surface tension, as quantified by the Bond number Eq. (2.3). The bubble in Figure 2C illustrates a schematic of one of these equilibrium shapes. The thin film separating the gas in the bubble from the gas outside the bubble is assumed to be of uniform thickness. Its overall shape is close to spherical, depending on the size of the bubble. This shape minimizes surface energy.

Once the bubble reaches its equilibrium surface shape, the liquid in its film drains back into the surrounding pool by a combination of gravitational draining and capillary suction; the relative strength of these draining mechanisms again depends on the Bond number or the size of the bubble. When small amounts of surfactant are present - as is the case for fluids containing biomass - the surfactant on the bubble's cap drains along with the liquid, leading to a gradient in surface tension (Stein 1993). The effect of this gradient is a Marangoni stress that counteracts the drainage (Fig. 3) and increases the persistence time of the bubble at the surface (Mysels et al. 1959). Regardless of the draining mechanism, the film eventually becomes thin enough for molecular forces to become destabilizing and cause rupture.

Indeed, the surface area of a bubble's thin shell is significantly greater than that of a spherical droplet of an identical volume of liquid. Thus, thin film caps are only local rather than global surface energy minima. In other words, small perturbations to a bubble's film surface area are attenuated. Yet, sufficiently large geometrical perturbation can lead to the development of a hole that will grow, resulting in the death or burst of the bubble. In particular, an initial hole can grow.

While the film remains thick enough, the initial hole can be induced by an external force

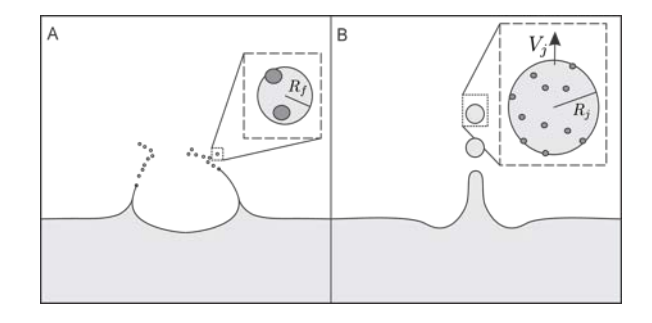


Figure 7. (A) Film drops and (B) jet drops can be a vector for biomaterial.

resulting from direct contact with solid objects or the deposition of dust particles. As thinning progresses. spontaneous popping eventually occur when the film's thickness becomes on the order of tens of nanometers. a scale at which Van der Waals forces are no longer negligible (Vrii 1966). However, such thickness is much smaller than that commonly observed prior to the burst of water bubbles with small surfactant concentrations, which is on the order of 0.1-10 micrometres. Once formed, the hole will grow if its size is larger than twice the thickness of the bubble film (Taylor & Michael 1973). Indeed, although it is unclear what initiates the rupture in these instances, experiments have demonstrated that the thickness of bubbles at burst decreases with decreasing surface tension and increases with size of the bubble, specifically $h \propto R^2$ (e.g. Modini et al. 2013 and references therein).

When a hole nucleates, its growth- or more precisely the retraction of the film - is driven by capillary forces due to the decrease in surface energy (Fig. 6). The dynamics of this retraction have been investigated for over a Dupré is credited for initially century. recognizing that when a hole nucleates in a thin sheet of liquid, the film around the hole collects into a growing rim while the rest of the film remains essentially still (Dupré 1867). By assuming that all of the surface energy released by the decrease in surface area is converted into the kinetic energy of the retracting rim, Dupré calculated that the film would retract at a constant velocity. results were echoed shortly later by Rayleigh

who carried out some of the earliest high-speed visualization (Rayleigh 1878), then again by De Vries (1958). Yet, more precise experiments by Ranz (1958) suggested that Dupré's calculation overestimated the velocity of retraction, motivating Culick (1960) to recognize that half of the surface energy is dissipated in the rim. Meanwhile, Taylor independently arrived at the same theoretical velocity while investigating retracting sheets (Taylor 1959).

Figure 6 illustrates the interaction of the retracting film with cells or other biologically relevant material. The relevant acceleration and the dissipation of energy experienced by these cells can be calculated by considering a force balance on the boundary of the retracting rim (dashed oval in Fig. 6). Assuming that the sheet is flat with width w, the capillary force F pulling on the rim is $2\gamma w$, where the factor of 2 is the result of there being an interface both above and below the film. This force is balanced by the change in momentum of the rim with respect to time. For a given velocity of retraction V, the mass of the rim increases at a rate of ρwhV , where ρ is the fluid's density and h is the film's thickness. Therefore, we arrive at constant retraction velocity $V = \sqrt{2\gamma / \rho h}$. The retraction velocity is identical for a spherical thin film geometry, as illustrated by Pandit & Davidson using both experiments (1990)calculations. For a 5-micrometre sheet of water, such retraction velocity is over 5 m/s. If particles were accelerated to this velocity over the distance of a 10-micrometre rim, the acceleration would be over 2×10^6 m/s², or 200,000 g. While this intense acceleration might be fatal for certain cells (Chalmers & Bavarian 1991), recent research suggests that many microorganisms can still thrive under such conditions (Deguchi et al. 2011).

6. A bubble's legacy lives on

Even following its death, a bubble can still impact its surroundings. Specifically, the rupture of the bubble can generate and disperse particulate-filled droplets (Fig. 7) as

well as create numerous smaller bubbles that themselves can rise to the surface and rupture. These droplets can persist in the air due to their small size, and have been linked to the transfer of pathogens (Parker et al. 1983; Embil et al. 1997; Falkinham 2003; Bourouiba & Bush 2012).

It was perhaps first Plateau (1873), upon reviewing the results of Dupré (1867), who recognized that the retracting rim of a bubble could become unstable and lead to the generation of hundreds of film drops (Fig. 7A). Particular attention has been given to the number and size of these film drops (e.g. Mason 1954; Day 1964; Afeti & Resch 1990; Spiel 1998) including when the film drops contained bacteria (Blanchard & Syzdek Numerous analytical and empirical relations have been proposed (e.g. Lewis & Schwartz 2004). For example, Mason (1954) reported 100-200 film droplets from bubbles of 0.5 to 3 mm diameter, while the number of film droplets for a bubble below 0.5 mm guickly decays (Lewis & Schwartz 2004) Perhaps some of the most convincing relations were proposed by Lhuissier & Villermaux (2011) who reasoned that the number $\,$ N and size $\,$ R $_{_{\mathbf{r}}}$ of film drops should scale as $N\sim \left(R/l_c\right)^2\left(R/h\right)^{7/8}$ and $R_{_f}\sim R^{3/8}\,h^{5/8}.$ Here R is the radius of the bubble, Ic is the capillary length, and h is the thickness of the bubble at rupture, assumed to range from 10-1000 micrometres. Surface tension and surfactants play a role in setting both the capillary length, as well as the thickness when the bubble bursts (Modini et al. 2013).

After the film has completed retracted, capillary forces rapidly close the remaining air cavity, often leading to the formation of a jet reminiscent of the classical Worthington jet (Worthington & Cole 1897). The jet rises upward and can become unstable; hence producing droplets (Fig. 7B). Such droplets are referred to as jet drops (Woodcock et al. 1953; F MacIntyre 1972; Blanchard 1989).

Experimental results demonstrate that the size of these jet drops R_i is approximately 5-20%

of the original bubble's radius R. For example, a so-called 10% rule was proposed by Kientzler et al. (1954) when observing up to 5 jet drops from bubbles of diameters ranging from 0.2 to 1.8 mm. Subsequent experiments developed more precise empirical relations between the sizes of jet droplets, their speeds and the original bubbles' sizes (e.g. Blanchard 1989; Spiel 1994; Spiel 1998; Lewis & Schwartz 2004). For a water bubble with a radius greater than 3 mm (Bo>1), capillary forces are not able to overcome the weight of the jet, and jet drops are seldom formed. Smaller bubbles - typically of less than 0.5 mm diameter – are observed to have more: yet at sufficiently small scales, viscous forces would eventually inhibit jet drops from forming. Indeed recent experiments using ultrafast Xray imaging have suggested that jets stop being produced at an Ohnesorge value of Oh ≈ 0.052, which would correspond to a water bubble of 4 micrometres in radius (Lee et al. 2011). Nevertheless, it has been argued that few jet drops at this scale would actually be produced on the ocean's surface, and even fewer would be dispersed into the atmosphere (Lewis & Schwartz 2004). In the event that a 5-micrometre bubble were to pop at the surface, the maximum height reached by its daughter jet drops would be only 400 micrometres (Blanchard 1989), thus limiting their ability to escape the boundary layer created by wind moving across the ocean surface.

The potential for a single bubble to generate both film drops and jet drops has long been appreciated (Knelman et al. 1954). Yet the relative number and sizes of these droplets tend to be quite different. As suggested by the scaling relations, larger bubbles (diameter above 3 mm) tend to be dominated by film drops, whereas smaller bubbles tend to be dominated by jet drops. Additionally, for a given bubble, film drops tend to be significantly smaller than jet drops.

Finally, in addition to creating droplets, a bubble can also create smaller, daughter bubbles as it ruptures (e.g. MacIntyre 1972; Herman & Mesler 1987; Bird et al. 2010).

These daughter bubbles can follow a similar life to their parent, rising, scavenging, and eventually rupturing; yet they carry out this progression while being at a smaller size. Therefore a bubble that may have been too large to create jet drops may generate numerous bubbles that each will propel numerous jet drops (and their contents) into the atmosphere.

7. Concluding remarks

From the open ocean to the shores; from indoor pools to bioreactors, bubbles are ubiquitous in bodies of water. As we see in this review, their role is multifaceted. Whether their role is desirable (e.g. for aeration or for transport of biomaterial) or harmful (e.g. outbreaks of disease along shores or indoors. or damage of cell cultures) bubbles deeply connect physics to biology through subtle interfacial fluid dynamics. Despite a relatively old identification of bubbles as physical and biological mixers and as creators of droplets, a range of fundamental questions pertaining to their interaction with the microorganismal world remain widely open. For example, the response of cells to sub-cellular level hydrodynamic forces is not understood; as performance is increased, non-lethal, negative effects may emerge (Hu et al. 2011). At the air-ocean interface does the stress of bubble damage certain organisms rupture observed in bioreactors thereby transmitting certain types or sizes selectively or more readily than others? In this brief review, we hope to have guided the reader through the rich life of a bubble and highlighted the many areas in which fluid dynamics can be of help in understanding bubbles; interactions with the world of the small.

Acknowledgements We thank the divisions within the Society of Integrative and Comparative Biology, including the Division of Comparative Biomechanics, the Division of Vertebrate Morphology, the Division of Invertebrate Zoology, and the American Microscopy Society for their support. LB is grateful for the financial support of NSF (1347346), and JCB is grateful for partial support from NSF CAREER award (1351466).

References

- Afeti, G.M. & Resch, F.J., 1990. Distribution of the liquid aerosol produced from bursting bubbles in sea and distilled water. *Tellus B*, 42B, pp.378–384.
- Angelini, T.E. et al., 2009. Bacillus subtilis spreads by surfing on waves of surfactant. *Proceedings of the National Academy of Sciences*, 106(43), pp.18109–18113.
- Baldy S. & Bourguel, M., 1987. Bubble between the wave trough and wave crest levels. *J. Geophys Res*, 92, pp.2919–2929.
- Barbosa, M.J., Albrecht, M. & Wijffels, R.H., 2003. Hydrodynamic stress and lethal events in sparged microalgae cultures. *Biotechnology and bioengineering*, 83(1), pp.112–20.
- Bauer, H. et al., 2002. Bacteria and fungi in aerosols generated by two different types of wastewater treatment plants. *Water research*, 36(16), pp.3965–70.
- Berg, J.C., Boudart, M. & Acrivos, A., 1966. Natural convection in pools of evaporating liquids. *J. Fluid Mech.*, 24, pp.721–735.
- Bhaga, D. & Weber, M.E., 1981. Bubbles in viscous liquids: shapes, wakes and velocities. *Journal of Fluid Mechanics*, 105, pp.61–85.
- Bird, J.C. et al., 2010. Daughter bubble cascades produced by folding of ruptured thin films. *Nature*, 465(7299), pp.759–762.
- Blanchard, D., 1989. The size and height to which jet drops are ejected from bursting bubbles in seawater. *Journal of Geophysical Research*, 94, pp.10,999–11,002.
- Blanchard, D. & Syzdek, L., 1972. Concentration of bacteria in jet drops from bursting bubbles. *Journal of Geophysical Research*, 77(27).
- Blanchard, D. & Syzdek, L., 1970. Mechanism for the water-to-air transfer and concentration of bacteria. *Science*, 170(3958), pp.626–628.
- Blanchard, D. & Syzdek, L., 1982. Water-to-air transfer and enrichment of bacteria in drops from bursting bubbles. *Applied and environmental microbiology*.
- Blanchard, D.C., 1963. The electrification of the atmosphere by particles from bubbles in the sea. *Progress in Oceanography*, 1(1254), pp.73–202.

- Blanchard, D.C. & Woodcock, A.H., 1957. Bubble formation and modification in the sea and its meteorological significance. *Tellus B*, 9, pp.145–158
- Boulton-Stone, J. & Blake, J., 1993. Gas bubbles bursting at a free surface. *Journal of Fluid Mechanics*.
- Bourouiba, L. & Bush, J.W.M., 2012. Drops and Bubbles in the Environment. In *Handbook of Environmental Fluid Dynamics*, *Volume One: Overview and Fundamentals*. CRC Press, pp. 427–440.
- Boyce, S.G., 1951. Source of Atmospheric Salts. *Science*, 113(2944), pp.620–621.
- Burger, S. & Bennett, J., 1985. Droplet enrichment factors of pigmented and nonpigmented Serratia marcescens: possible selective function for prodigiosin. *Applied and environmental microbiology*, 50(2).
- Chalmers, J.J. & Bavarian, F., 1991. Microscopic visualization of insect cell-bubble interactions. II: The bubble film and bubble rupture. *Biotechnology progress*, 7(2), pp.151–158.
- Cherry, R. & Hulle, C., 1992. Cell death in the thin films of bursting bubbles. *Biotechnology progress*, pp.11–18.
- Chisti, Y., 2000. Animal-cell damage in sparged bioreactors. *Trends in biotechnology*, 18(10), pp.420–432.
- Clift, R., Grace, J.R. & Weber, M.E., 1978. *Bubbles, drops, and particles*, Acedemic Press, Inc.
- Culick, F., 1960. Comments on a ruptured soap film. Journal of Applied Physics.
- Czerski, H. et al., 2011. Resolving size distributions of bubbles with radii less than 30 µ m with optical and acoustical methods. *Journal of Geophysical Research*, 116(November), p.C00H11.
- Dai, Z., Fornasiero, D. & Ralston, J., 2000. Particlebubble collision models--a review. Advances in colloid and interface science, 85(2-3), pp.231–56.
- Day, J.A., 1964. Production of droplets and salt nuclei by the bursting of air-bubble films. Quarterly Journal of the Royal Meteorological Society, 90(383), pp.72–78.

- Deane, G.B. & Stokes, M.D., 2002. Scale dependence of bubble creation mechanisms in breaking waves. *Nature*, 418(6900), pp.839–44.
- Deguchi, S. et al., 2011. Microbial growth at hyperaccelerations up to 403,627 x g. *Proceedings of the National Academy of Sciences of the United States of America*, 108(19), pp.7997–8002.
- Dupré, A., 1867. Sixieme memoire sur la theorie mécanique de la chaleur. *Ann. Chim. Phys.*, 11, pp.194–220.
- Embil, J. et al., 1997. Pulmonary Illness Associated With Exposure to Mycobacterium-avium Complex in Hot Tub Water* Hypersensitivity Pneumonitis or Infection? *CHEST Journal*, 111(3), pp.813–816.
- Falkinham III, J.O., 2003. Mycobacterial aerosols and respiratory disease. *Emerging infectious diseases*, 9(7), pp.763–7.
- Garcia-Briones, M.A. & Chalmers, J.J., 1994. Flow parameters associated with hydrodynamic cell injury. *Biotechnology and bioengineering*, 44(9), pp.1089–1098.
- Gong, X. et al., 2007. A numerical study of mass transfer of ozone dissolution in bubble plumes with an Euler-Lagrange method. *Chemical Engineering Science*, 62(4), pp.1081–1093.
- Hadamard, J., 1911. Mouvement permanent lent d'une sphere liquide et visqueuse dans un liquide visqueux. *CR Acad. Sci*, 152(25), pp.1735–1738.
- Herman, J. & Mesler, R., 1987. Bubble entrainment from bursting bubbles. *Journal of colloid and interface science*, 117(2), pp.565–569.
- Hosoi, A.E. & Bush, J.W.M., 2001. Evaporative instabilities in climbing films. *Journal of fluid Mechanics*, 442, pp.217–239.
- Hu, W., Berdugo, C. & Chalmers, J.J., 2011. The potential of hydrodynamic damage to animal cells of industrial relevance: current understanding. *Cytotechnology*, 63(5), pp.445–60.
- Jacobs, W., 1937. Preliminary report on a study of atmospheric chlorides. *Monthly Weather Review*, (April).
- Kientzler, C. et al., 1954. Photographic Investigation of the Projection of Droplets by Bubbles Bursting at a Water Surface1. *Tellus*, pp.1–7.

- Knelman, F., Dombrowski, N. & M. Newitt, D., 1954. Mechanism of the bursting of bubbles. *Nature*, 4397, p.261.
- Kumar, R. & Kuloor, N.R., 1970. The formation of bubbles and drops. *Advances in chemical engineering*, 8, pp.255–368.
- Laitinen, S. et al., 1994. Workers' exposure to airborne bacteria and endotoxins at industrial wastewater treatment plants. *American Industrial Hygiene Association*, 55(11), pp.1055–1060.
- Lee, J.S. et al., 2011. Size limits the formation of liquid jets during bubble bursting. *Nature communications*, 2, p.367.
- Lewis, R. & Schwartz, E., 2004. Sea salt aerosol production: mechanisms, methods, measurements and models—a critical review, American Geophysical Union.
- Lhuissier, H. & Villermaux, E., 2011. Bursting bubble aerosols. *Journal of Fluid Mechanics*, 696, pp.5–44
- Liu, Y. et al., 2013. Effects of bubble-liquid two-phase turbulent hydrodynamics on cell damage in sparged bioreactor. *Biotechnology progress*, pp.1–11.
- MacIntyre, F., 1972. Flow patterns in breaking bubbles. Journal of Geophysical Research.
- MacIntyre, F., 1972. Flow patterns in breaking bubbles. *Journal of Geophysical Research*, 77(27), pp.5211–5228.
- Magnaudet, J. & Eames, I., 2000. The motion of high-Reynolds-number bubbles in inhomogeneous flows. *Annual Review of Fluid Mechanics*, pp.659– 708.
- Maier, C.G., 1927. The Ferric Sulphate-Sulphuric Acid Process: With a Chapter on Producing Small Bubbles of Gas in Liquids by Submerged Orifices,
- Marangoni, C., 1865. On the expansion of a drop of liquid floating on the surface of another liquid. Tipographia dei fratelli Fusi, Pavia.
- Mason, B.J., 1954. Bursting of air bubbles at the surface of sea water.
- Meier, S.J., Hatton, T. a & Wang, D.I., 1999. Cell death from bursting bubbles: role of cell attachment to rising bubbles in sparged reactors. *Biotechnology and bioengineering*, 62(4), pp.468–78.

- Melville, W.K., 1996. The role of surface-wave breaking in air-sea interaction. *Annual review of fluid mechanics*, 28(1), pp.279–321.
- Miettinen, T., Ralston, J. & Fornasiero, D., 2010. The limits of fine particle flotation. *Minerals Engineering*, 23(5), pp.420–437.
- Miyahara, T. & Hayashino, T., 1995. Size of bubbles generated from perforated plates in non-Newtonian liquids. *Journal of chemical engineering of Japan*, 28(5), pp.596–600.
- Modini, R.L. et al., 2013. Effect of soluble surfactant on bubble persistence and bubble-produced aerosol particles. *Journal of Geophysical Research: Atmospheres*, 118(3), pp.1388–1400.
- Monahan, E., 1971. Oceanic whitecaps. *Journal of Physical Oceanography*.
- Mulhearn, P.J., 1981. Distribution of microbubbles in coastal waters. *Journal of Geophysical Research*, 86(C7), p.6429.
- Murhammer, D.W. & Goochee, C.F., 1990. Sparged animal cell bioreactors: mechanism of cell damage and Pluronic F-68 protection. *Biotechnology progress*, 6(5), pp.391–7.
- Mysels, K.J., Shinoda, K. & Frankel, S., 1959. Soap films: studies of their thinning and a bibliography, Pergamon press.
- Pandit, A. & Davidson, J., 1990. Hydrodynamics of the rupture of thin liquid films. *J. Fluid Mech*.
- Parker, B.C. et al., 1983. Epidemiology of infection by nontuberculous mycobacteria. IV. Preferential aerosolization of Mycobacterium intracellulare from natural waters. *The American review of respiratory disease*, 128(4), pp.652–656.
- Plateau, J., 1873. Experimental and theoretical statics of liquids subject to molecular forces only. *Gauthier-Villars, Paris*.
- Ranz, W.E., 1958. Some experiments on the dynamics of liquid films. *J. Appl. Phys.*, 30, pp.1950–1955.
- Rayleigh, L., 1878. On the instability of jets. *Proceedings* of the London Mathematical Society, pp.4–12.
- Rybczynski, W., 1911. On the translatory motion of a fluid sphere in a viscous medium. *Bull Acad Sci Cracow Ser A*, 40, pp.40–46.

- Schulze, H.J., 1992. Probability of particle attachment on gas bubbles by sliding. *Advances in Colloid and Interface Science*, 40, pp.283–305.
- Scriven, L.E. & Sternling, C. V, 1960. The marangoni effects. *Nature*, pp.186–188.
- Spiel, D., 1994. The sizes of the jet drops produced by air bubbles bursting on sea- and fresh-water surfaces. *Tellus B*.
- Spiel, D.E., 1998. On the births of film drops from bubbles bursting on seawater surfaces. *Journal of Geophysical Research: Oceans (1978--2012)*, 103(C11), pp.24907–24918.
- Stein, H.N., 1993. The drainage of free liquid films. Colloids and Surfaces A: Physicochemical and Engineering Aspects, 79(1), pp.71–80.
- Stuhlman, O., 1932. The Mechanics of Effervescence. *Physics*, 2(6), p.457.
- Sullivan, S.L., Hardy, B.W. & Holland, C.D., 1964.
 Formation of air bubbles at orifices submerged beneath liquids. AIChE Journal, 10(6), pp.848–854
- Sutherland, K., 1948. Physical chemistry of flotation. XI. Kinetics of the flotation process. *The Journal of Physical Chemistry*, (5).
- Takemura, F. & Yabe, a., 1999. Rising speed and dissolution rate of a carbon dioxide bubble in slightly contaminated water. *Journal of Fluid Mechanics*, 378, pp.319–334.
- Taylor, G., 1959. The dynamics of thin sheets of fluid. III. Disintegration of fluid sheets. *Proceedings of the Royal Society of London*, 253(1274), pp.313–321.
- Taylor, G.I. & Michael, D.H., 1973. On making holes in a sheet of fluid. *J. Fluid Mech.*, 58(04), pp.625–639.
- Thoroddsen, S.T., Etoh, T.G. & Takehara, K., 2007. Experiments on bubble pinch-off. *Physics of Fluids*, 19(4), p.042101.
- Tramper, J. et al., 1986. Shear sensitivity of insect cells in suspension. *Enzyme and microbial* ..., 8, pp.33–36.
- Verrelli, D.I., Koh, P.T.L. & Nguyen, A. V., 2011. Particle–bubble interaction and attachment in flotation. *Chemical Engineering Science*, 66(23), pp.5910–5921.

- De Vries, A.J., 1958. Foam stability: Part IV. Kinetics and activation energy of film rupture. *Recueil des travaux chimiques des Pays-Bas*, 77(4), pp.383–399.
- Vrij, A., 1966. Possible mechanism for the spontaneous rupture of thin, free liquid films. *Discuss. Faraday* Soc., pp.23–33.
- Wallace, G., Loeb, G. & Wilson, D., 1972. On the flotation of particulates in sea water by rising bubbles. *Journal of Geophysical Research*, 77(27), pp.5293–5301.
- Weber, M., Blanchard, D. & Syzdek, L., 1983. The mechanism of scavenging of waterborne bacteria by a rising bubble. *Limnology and Oceanography*, 28(1), pp.101–105.
- Wernersson, E.S. & Trägårdh, C., 1999. Scale-up of Rushton turbine-agitated tanks. *Chemical engineering science*, 54.
- Woodcock, A. et al., 1953. Giant condensation nuclei from bursting bubbles. *Nature*.
- Woodcock, A.H.A., 1948. Note concerning human respiratory irritation associated with high concentrations of plankton and mass mortality of marine organisms. *J Mar Res*, 7(1), pp.56–62.
- Worthington, A.M. & Cole, R.S., 1897. Impact with a liquid surface, studied by the aid of instantaneous photography. *Philosophical Transactions of the Royal Society of London. Series A, Containing Papers of a Mathematical or Physical Character*, pp.137–148.
- Wurl, O. et al., 2011. Formation and global distribution of sea-surface microlayers. *Biogeosciences*, 8(1), pp.121–135.
- Yoon, R.H. & Luttrell, G.H., 1989. The effect of bubble size on fine particle flotation. *Mineral Processing and Extractive Metallurgy Review*, 5(1-4), pp.101–122.
- Zhu, Y. et al., 2008. NS0 cell damage by high gas velocity sparging in protein-free and cholesterol-free cultures. *Biotechnology and bioengineering*, 101(4), pp.751–60.
- Žutić, V. et al., 1981. Surfactant production by marine phytoplankton. *Marine Chemistry*, 10(6), pp.505– 520.